frontiers | Frontiers in Energy Research

TYPE Original Research
PUBLISHED 29 August 2022
DOI 10.3389/fenrg.2022.978819

OPEN ACCESS

EDITED BY
Adnan,
Mohi-ud-Din Islamic University, Pakistan

REVIEWED BY
Ali Akgül,
Siirt University, Turkey
Siti Suzilliana Putri Mohamed Isa,
Putra Malaysia University, Malaysia

*CORRESPONDENCE
Sohail Ahmad,
sohailkhan1058@gmail.com

SPECIALTY SECTION
This article was submitted to Process and Energy Systems Engineering, a section of the journal Frontiers in Energy Research

RECEIVED 26 June 2022
ACCEPTED 21 July 2022
PUBLISHED 29 August 2022

CITATION
Ahmad S, Ali K, Haider T, Jamshed W, Tag El Din ESM and Hussain SM (2022), Thermal characteristics of kerosene oil-based hybrid nanofluids (Ag-$MnZnFe_2O_4$): A comprehensive study. *Front. Energy Res.* 10:978819. doi: 10.3389/fenrg.2022.978819

Thermal characteristics of kerosene oil-based hybrid nanofluids (Ag-$MnZnFe_2O_4$): A comprehensive study

Sohail Ahmad[1]*, Kashif Ali[2], Tahir Haider[3], Wasim Jamshed[4], El Sayed M. Tag El Din[5] and Syed M. Hussain[6]

[1]Centre for Advanced Studies in Pure and Applied Mathematics (CASPAM), Bahauddin Zakariya University, Multan, Pakistan, [2]Department of Basic Sciences and Humanities, Muhammad Nawaz Sharif University of Engineering and Technology, Multan, Pakistan, [3]Punjab Danish School and Centre of Excellence (Boys), Dera Ghazi Khan, Pakistan, [4]Department of Mathematics, Capital University of Science and Technology, Islamabad, Pakistan, [5]Electrical Engineering, Faculty of Engineering and Technology, Future University in Egypt, New Cairo, Egypt, [6]Department of Mathematics, Faculty of Science, Islamic University of Madinah, Medina, Saudi Arabia

Hybrid nanofluids are new and most fascinating types of fluids that involve superior thermal characteristics. These fluids exhibit better heat-transfer performance as equated to conventional fluids. Our concern, in this paper, is to numerically interpret the kerosene oil-based hybrid nanofluids comprising dissimilar nanoparticles like silver (Ag) and manganese zinc ferrite ($MnZnFe_2O_4$). A numerical algorithm, which is mainly based on finite difference discretization, is developed to find the numerical solution of the problem. A numerical comparison appraises the efficiency of this algorithm. The effects of physical parameters are examined via the graphical representations in either case of nanofluids (pure or hybrid). The results designate that the porosity of the medium causes a resistance in the fluid flow. The enlarging values of nanoparticle volume fraction of silver sufficiently increase the temperature as well as velocity. It is examined here that mixture of hybrid nanoparticles (Ag-$MnZnFe_2O_4$) together with kerosene oil can provide assistance in heating up the thermal systems.

KEYWORDS

manganese zinc ferrite, silver, kerosene oil, Darcy Forchheimer medium, activation energy

Introduction

Kerosene oil-based hybrid nanofluids can embellish the thermal characteristics; that is why these fluids have several uses in modern engineering and technology (Upreti et al., 2021; Yahya et al., 2022). The host or base fluid such as kerosene oil also plays an important role in augmentation of the heat-transfer performance rather than the nanoparticles. A combustible hydrocarbon-type liquid often obtained from petroleum can be referred to as kerosene oil, which is also known as paraffin or lamp oil. It is used as jet fuel in jet engines, as lighting and cooking fuel, as aviation fuel, as an oil-based paint,

and in corrosion experiments. Due to these characteristics, we have chosen kerosene oil as the host fluid in the current analysis. To prepare the hybrid composition (Ahmad et al., 2021a), nanoparticles of manganese zinc ferrite and silver are mixed in kerosene oil. Silver is a metal or chemical element having the highest thermal and electrical conductivity as compared to other metals. It is usually found in Earth's crust as a free element. Many substances are made of silver, such as ornaments, jewellery, utensils, solar panels, high-value tableware, and lead, and it is used in stained glass, catalysis of chemical reactions, window coatings, specialized mirrors, zinc refining, gold, and so forth. Manganese zinc ferrites belong to ferrite materials and exhibit high magnetic permeability (Ahmad et al., 2022a). These are widely used in noise filters, choke coils, transformers, and memory devices. Some recent investigations on nanofluids and hybrid nanofluids are discussed in reference articles (Abdal et al., 2021; Ahmad et al., 2021b; Zahid et al., 2021; Ayub et al., 2022; Nisar et al., 2022; Safdar et al., 2022).

Recently, many researchers have evaluated the thermal performance of usual and hybrid nanofluids numerically, theoretically, and experimentally. Dawar et al. (2022) investigated the kerosene oil and water-based hybrid nanofluid flow of copper and copper oxide nanoparticles. The magnetohydrodynamic effect was also taken into account, and the flow was taken over a bi-directional expanding surface. Comparative results of both hybrid nanofluids were established. The hybrid mixture of copper and aluminum oxide particles was prepared to form water-based hybrid nanofluid flow of Cu-Al_2O_3/water (Zainal et al., 2022). The outcomes of this study revealed that the Nusselt number got reduced when the values of slip parameter increased. Akhter et al. (2022) and Ali et al. (2022) numerically simulated the nanofluid and hybrid nanofluid flows using the quasilinearization technique, respectively. Ezhil et al. (2021) presented the analysis of ferrous oxide Fe_3O_4 and copper (Cu) taking ethylene glycol as the base fluid. Flow was assumed to be fully developed occurring over a stretching sheet. The same work was carried out by Unyong et al. (2022) taking the effects of an inclined magnetic field and partial slip.

Heat transmission and fluid flow in permeable media have gained utmost attention of researchers due to their practical employments. Flow of Williamson nanofluids over a horizontal sheet embedded in a porous medium taking the combined impact of Brownian motion and thermal radiation was studied by Mishra and Mathur (2020). A boundary layer flow involving gyrotactic microorganisms and nanofluids was examined by Elbashbeshy and Asker (2022). The nonlinear velocity caused the stretching of sheets, and the controlling parameters were discussed quantitatively. The characteristics of flow dynamics in porous media and in the presence of nanoparticles have substantial effects on heat-transfer effects (Dastvareh and Azaiez, 2017). In this paper, it was determined that nanoparticles decreased the viscosity

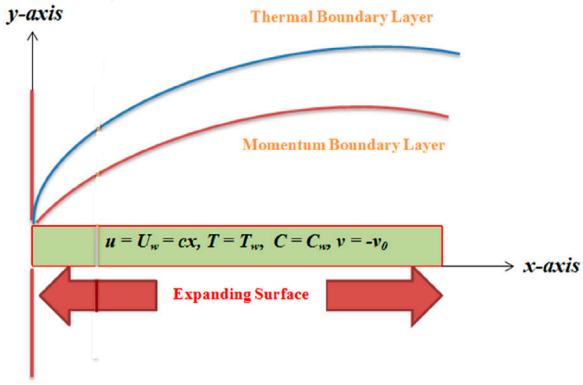

FIGURE 1
Structure of the geometry.

distribution monotonically. Flow and heat transfer of ferro-nanofluids through Darcian porous media between channel walls were numerically simulated by Das et al. (2019). The heat-transfer rate at the upper channel wall was noticed to be increasing as compared to the lower wall. Flow of nanoparticles in the presence of peristaltic waves and porous media has been investigated by Kareem and Abdulhadi (2020). They achieved numerical results using the Mathematica 11 program. More recent numerical investigations on nanofluids can be found in Ahmed et al., 2017a; Ahmed et al., 2017b; Ahmed et al., 2018; Ahmed et al., 2020; Adnan et al., 2022a; Adnan et al., 2022e; Adnan et al., 2022f; Adnan et al., 2022b; Adnan et al., 2022d; and Adnan et al., 2022c.

In spite of so much efforts to explore and discover the new energy sources, still, struggle is continued. New types of hybrid nanocompositions are being introduced. The available literature evidently discloses that kerosene oil-based nanofluids and hybrid nanofluids consisting of silver (Ag) and manganese zinc ferrite ($MnZnFe_2O_4$) nanoparticles have not been numerically investigated yet. However, our analysis is a first effort to examine the nanocomposition of Ag-$MnZnFe_2O_4$-KO. The role of chemical reaction, suction, and porous media is also discussed in both pure and hybrid cases of nanofluids. Numerical solutions are found with the help of finite difference discretization via MATLAB. Thermal systems can manage and maintain their temperature and heat-transfer rate with the help of proposed hybrid compositions, for example, Ag-$MnZnFe_2O_4$-KO.

Problem formulation

The nanoparticles of silver (Ag) and manganese zinc ferrite ($MnZnFe_2O_4$) are mixed in kerosene oil to form the hybrid nanocomposite of Ag-$MnZnFe_2O_4$/kerosene oil. The *x*- and

TABLE 1 Thermal properties of silver, kerosene oil, and manganese zinc ferrite.

Properties	Ag (s_2)	Kerosene oil (f)	$MnZnFe_2O_4$ (s_1)
k (W/mK)	429.0	0.145	3.9
C_p (J/kgK)	235.00	2090.0	1050
ρ (kg/m^3)	10500.0	783.0	4700

y-axes are taken in such a way that the fluid flowing along the x-axis and y-axis is vertical to the surface. Figure 1 demonstrates the structure of the extending surface. It is assumed that the fluid is flowing through a porous medium with the effect of chemical reaction.

The model governing equations have the following form (Ahmad et al., 2021c):

$$\frac{\partial u}{\partial x}+\frac{\partial v}{\partial y}=0 \tag{1}$$

$$u\frac{\partial u}{\partial x}+v\frac{\partial u}{\partial y}=\upsilon_{hnf}\frac{\partial^2 u}{\partial y^2}-\frac{\mu_{hnf}}{\rho_{hnf}k^*}u \tag{2}$$

$$u\frac{\partial T}{\partial x}+v\frac{\partial T}{\partial y}=\frac{K_{hnf}}{\left(\rho C_p\right)_{hnf}}\frac{\partial^2 T}{\partial y^2} \tag{3}$$

$$u\frac{\partial C}{\partial x}+v\frac{\partial C}{\partial y}=D_B\frac{\partial^2 C}{\partial y^2}-K_r\left(C-C_\infty\right). \tag{4}$$

The analogous boundary conditions (BCs) are

$$\left.\begin{array}{l} y=0:\ u(x,0)=U_w(x)=cx, T(x,0)=T_w, v(x,0)=-v_0, C(x,0)=C_w \\ y\to\infty: u(x,\infty)=0, T(x,\infty)=T_\infty, C(x,\infty)=C_\infty \end{array}\right\} \tag{5}$$

The suction velocity is denoted by $v_0>0$. The notations T_w and T_∞ represent the temperatures at the surface boundary and away from the boundary. Likewise, the concentrations away from the boundary and at the boundary are respectively represented by C_∞ and C_w. The surface is stretching with the velocity $U_w(x)=u(x,0)=cx$ The hybrid nanofluid is expressed by the notation hnf.

Formation of pure (Ag/KO) and hybrid nanofluids ($MnZnFe_2O_4$-Ag/KO)

The hybrid nanocomposite $MnZnFe_2O_4$-Ag/KO can be achieved by mixing the nanoparticles of manganese zinc ferrite ($MnZnFe_2O_4$) and silver (Ag) in the kerosene oil (KO). Initially, the volume fraction of $MnZnFe_2O_4$ (ϕ_1) is considered as 0.2 when resolved in the kerosene oil to form the pure nanofluid $MnZnFe_2O_4$/KO. Afterward, the particles of Ag (ϕ_2) are inserted in this solution, which give rise to the hybrid nanofluids ($MnZnFe_2O_4$-Ag/KO). Thermal properties of manganese zinc ferrite, silver, and kerosene oil are specified in Table 1. Further characteristics like specific heat, thermal conductivity, and density (in both cases of nanofluids) are assumed to be the same as those taken by Ahmad et al. (2021d). The notation s_2 expresses the silver volume fraction, and s_1 is used for the volume fraction of manganese zinc ferrite. The host fluid kerosene oil is represented by f.

Dimensionless variables

The following dimensionless variables are introduced in order to convert partial differential equations (PDEs) into a dimensionless system of ordinary differential equations (ODEs):

$$\xi=\sqrt{\frac{c}{\upsilon_f}}y,\ \psi=\sqrt{c\upsilon_f}xf(\xi),\ \theta(\xi)=\frac{T-T\infty}{T_w-T\infty},\ \phi(\xi)=\frac{C-C_\infty}{C_w-C_\infty} \tag{6}$$

The continuity equation (Eq. 1) is identically satisfied by relation (6), and this relation renovates the system of Eqs. 2–4 in the form

$$f'''=\Delta_1\left(f'^2-ff''\right)+\varepsilon f' \tag{7}$$

$$\frac{1}{\Pr}\Delta_2\theta''+\Delta_3 f\theta'=0 \tag{8}$$

$$\frac{1}{Sc}\phi''+f\phi'-C_R\phi=0 \tag{9}$$

where

$$\Delta_1=\left(1-\phi_1\right)^{2.5}\left(1-\phi_2\right)^{2.5}\left[\left(1-\phi_2\right)\left\{\left(1-\phi_1\right)+\phi_1\frac{\rho_{s_1}}{\rho_f}\right\}+\phi_2\frac{\rho_{s_2}}{\rho_f}\right] \tag{10}$$

$$\Delta_2=\frac{K_{hnf}}{K_f} \tag{11}$$

$$\Delta_3=\left[\left(1-\phi_2\right)\left\{\left(1-\phi_1\right)+\phi_1\frac{\left(\rho c_p\right)_{s_1}}{\left(\rho c_p\right)_f}\right\}+\phi_2\frac{\left(\rho c_p\right)_{s_2}}{\left(\rho c_p\right)_f}\right] \tag{12}$$

The BCs (5) take the following form now:

$$\left.\begin{array}{l} \xi=0:\ f=\lambda_S, f'=1, \theta=1, \phi=1, \\ \xi\to\infty: f'\to 0, \theta\to 0, \phi\to 0. \end{array}\right\} \tag{13}$$

Problem parameters

The problem parameters of dimensionless Eqs. 7–9 are identified as follows:

$S_c=\frac{\upsilon_f}{D_B}$ is the Schmidt number

$\lambda_S=\frac{v_0}{\sqrt{c\upsilon_f}}$ is the suction parameter

$\Pr=\frac{\mu_f(c_p)_f}{k_f}$ is the Prandtl number

$\varepsilon=\frac{\upsilon_f}{ck^*}$ is the porosity parameter

$C_R=\frac{K_r^2}{c}$ is the chemical reaction parameter

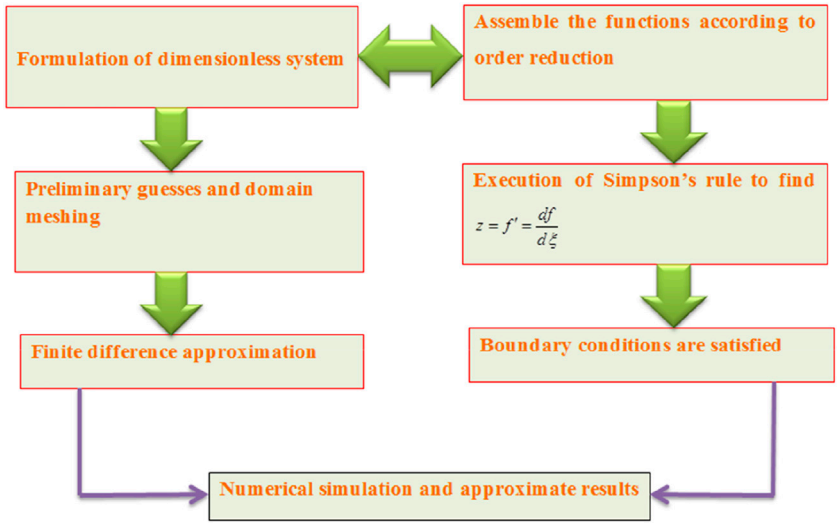

FIGURE 2
Flow chart of the numerical method.

The relations for shear stress as well as Sherwood and Nusselt number are given by

$$\mathrm{Re}_x^{\frac{1}{2}} C_{fx} = \frac{f''(0)}{(1-\phi_1)^{2.5}(1-\phi_2)^{2.5}}, Sh_x \mathrm{Re}_x^{\frac{1}{2}} = -\phi'(0),$$

$$Nu_x \mathrm{Re}_x^{\frac{1}{2}} = -\frac{k_{hnf}}{k_f}\theta'(0). \tag{14}$$

whereas the local Reynolds number is given as $\mathrm{Re}_x = \frac{U_w x}{\upsilon_f}$.

Numerical scheme based on finite difference discretization

Finding the analytical solution of the coupled Eqs. 7–9 may be so much time-consuming as these equations are not only higher-order but also highly nonlinear. However, we require some persuasive numerical technique which could be employed to determine the solution of the problem. Therefore, we adopt a finite difference methodology in order to find the numerical solution of the problem under consideration. The different numerical methods (to solve such types of dynamical problems) that we adopted in our earlier work can be seen in reference articles (Ahmad et al., 2021e; Ahmad et al., 2021f; Jamshed. et al., 2021; Ahmad et al., 2022b). We describe the structure of this methodology in the following flow chart diagram (Figure 2).

Results and discussion

This section depicts the analysis of mono (Ag/kerosene oil) and hybrid (Ag-$MnZnFe_2O_4$/kerosene oil) cases of nanofluids. The nanocomposites of silver (Ag) into the kerosene oil give rise to the mono nanofluid, whereas the amalgamation of manganese zinc ferrite and silver produces the hybrid mixture. The effects of physical parameters are deliberated via the graphs and tables. Table 2 portrays a comparison which is found to be in a good correlation with the existing outcomes under limiting cases.

TABLE 2 Change in heat-transfer rate for different Prandtl numbers when $\phi_1 = \phi_2 = 0$.

Pr	Literature results (Khan and Pop, 2010)	Present results
2	0.9113	0.91045
7	1.8954	1.89083
20	3.3539	3.35271
70	6.4621	6.47814

TABLE 3 Impact of porosity parameter on $\mathrm{Re}_x^{\frac{1}{2}} C_f$ and $\mathrm{Re}_x^{-\frac{1}{2}} Nu_x$.

	$\mathrm{Re}_x^{\frac{1}{2}} C_f$		$\mathrm{Re}_x^{-\frac{1}{2}} Nu_x$	
ε	Ag/KO	Ag-$MnZnFe_2O_4$/KO	Ag/KO	Ag-$MnZnFe_2O_4$/KO
1.2	-4.1328499	-6.8013631	9.8973507	13.7221408
2.2	-4.3509353	-7.1978370	9.8899404	13.7081393
3.3	-4.5731705	-7.5998153	9.8825911	13.6943887
4.2	-4.7438059	-7.9072949	9.8770823	13.6841633

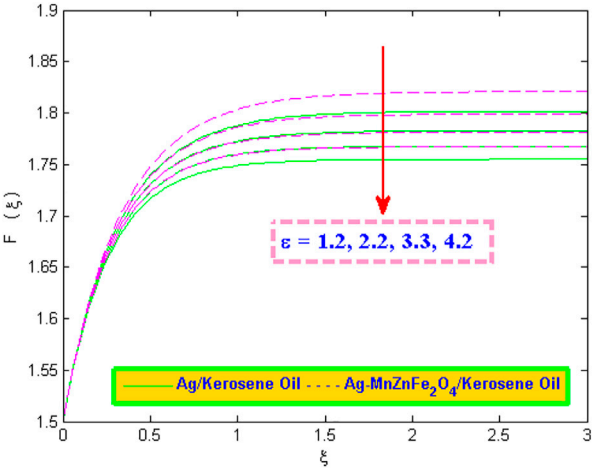

FIGURE 3
Variation in velocity with ε.

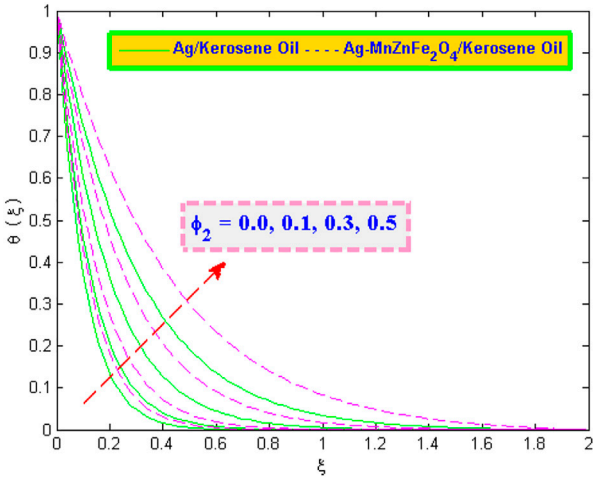

FIGURE 5
Variation in temperature with ϕ_2.

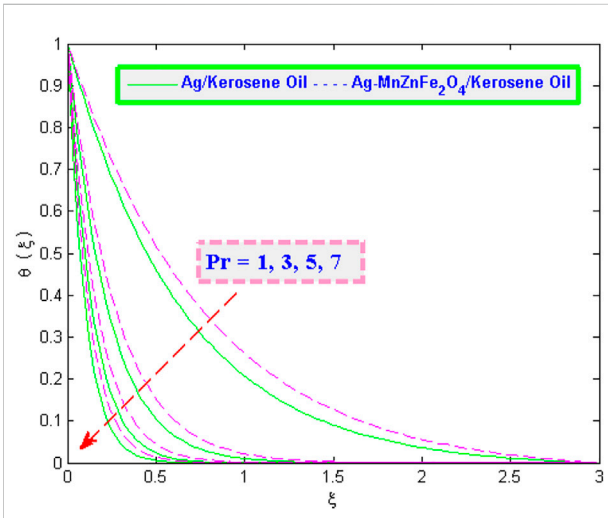

FIGURE 4
Variation in temperature with *pr*.

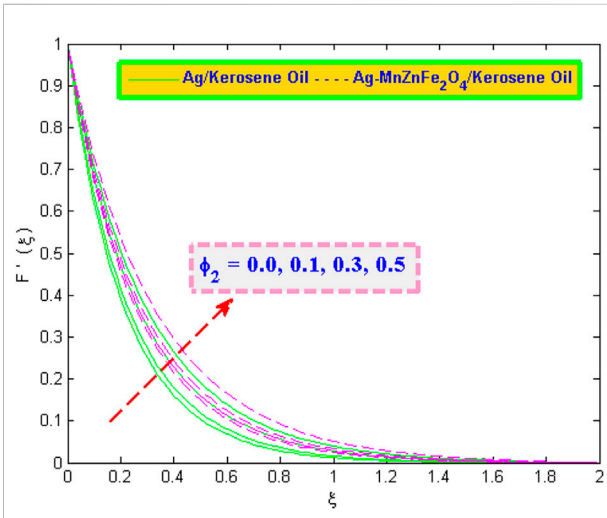

FIGURE 6
Variation in velocity with ϕ_2.

TABLE 4 Impact of nanoparticle volume fraction and Prandtl number on $\mathrm{Re}_x^{-1/2} Nu_x$.

	$\mathrm{Re}_x^{-1/2} Nu_x$			$\mathrm{Re}_x^{-1/2} Nu_x$	
ϕ_2	Ag/KO	Ag-$MnZnFe_2O_4$/KO	*Pr*	Ag/KO	Ag-$MnZnFe_2O_4$/KO
0.0	9.6014532	13.5632834	1	1.8078974	2.5876586
0.1	10.1558546	13.8085327	3	4.9757331	6.8999489
0.3	11.3109163	14.3420655	5	8.1204811	11.2517676
0.5	12.6458643	15.1546670	7	11.2068343	15.5277464

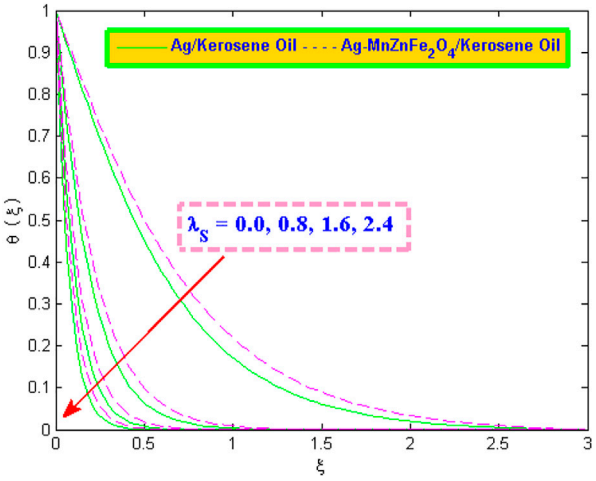

FIGURE 7
Variation in temperature with λ_s

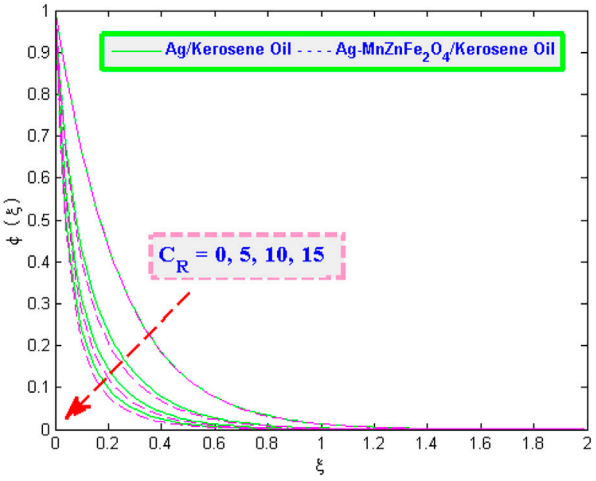

FIGURE 9
Variation in concentration with C_R.

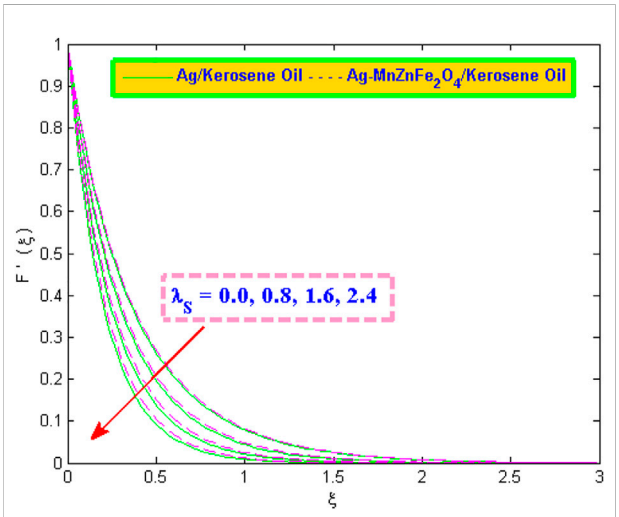

FIGURE 8
Variation in velocity with λ_s.

We assign fixed values to the parameters such as Pr = 6.135. The other specified values which have been used in finding the numerical solution are

$$\varepsilon = 4, \phi_1 = 0.2, Sc = 2.5, \phi_2 = 0.05, \lambda_s = 1.5, C_R = 4.$$

The change in surface drag $\mathrm{Re}_x^{\frac{1}{2}} C_f$ and Nusselt number $\mathrm{Re}_x^{-\frac{1}{2}} Nu_x$ against porosity parameter ε can be observed from Table 3. An increase in the values of porosity parameter tends to enhance the skin friction, but its effect is to deteriorate the rate of heat transfer. The fluid flow is resisted by the porosity of the medium due to which the velocity of the fluid reduces (see Figure 3). The Prandtl number tends to deteriorate the temperature as shown in Figure 4.

Thermal characteristics in either case of nanofluids are affected by the volume fraction ϕ_2 of silver nanoparticles. The required outcomes can be attained by suitably taking the volume fractions of nanoparticles. It is comparatively noticed from Figure 5 that the temperature increases rapidly in the case of

TABLE 5 Impact of activation energy and chemical reaction on $\mathrm{Re}_x^{-\frac{1}{2}} Sh_x$.

	$\mathrm{Re}_x^{-\frac{1}{2}} Nu_x$			$\mathrm{Re}_x^{-\frac{1}{2}} Sh_x$	
λ_S	Ag/KO	Ag-$MnZnFe_2O_4$/KO	C_R	Ag/KO	Ag-$MnZnFe_2O_4$/KO
0.0	1.4868709	2.1831767	0	4.0539553	4.0604246
0.8	5.7505953	8.0283592	5	10.5963505	4.0604246
1.6	10.4093347	14.4429463	10	14.8876215	15.5156646
2.4	15.0452404	20.8890408	15	18.1589037	18.8270273

the hybrid composition Ag-$MnZnFe_2O_4$/KO rather than the composition of Ag/KO when we increase the volume concentration ϕ_2. In the same way, the velocity of the fluid accelerates quickly in the hybrid case of the nanofluid as pictured in Figure 6. The impact of both volume fraction ϕ_2 and the Prandtl number Pr is to escalate the Nusselt number $\mathrm{Re}_x^{-\frac{1}{2}} Nu_x$ for both pure and hybrid nanofluids (see Table 4).

The variation in temperature and velocity for diverse values of the suction parameter can be examined from Figures 7, 8. Both the temperature $\theta(\xi)$ and velocity $F'(\xi)$ turn toward reduction (in both cases of nanofluids) with the effect of suction. Figure 9 illustrates the influence of the chemical reaction parameter on concentration in either case of the nanofluid. A decreasing trend is noticed in the concentration profile, which shows that the chemical reaction parameter C_R causes a substantial decrease in the concentration.

The mass-transfer rate increases with an increase in the values of C_R as observed in Table 6. It has also been deduced from Table 5 that the suction parameter λ_S marginally enhances the heat-transfer rate in the case of the hybrid nanofluid Ag-$MnZnFe_2O_4$/KO rather than the usual case of the nanofluid Ag/KO.

Conclusion

Specific rate of heat transfer plays an important role in many engineering systems as it can affect the quality of the product. A certain or specific heat-transfer rate is essentially required in many energy systems, for example, metal expulsion, nuclear system cooling, refrigeration, thermal storage, cooling generator, and so on. The amalgamation of manganese zinc ferrites ($MnZnFe_2O_4$) and silver (Ag) in kerosene oil can provide assistance in increasing the heat-transfer rate. The main results of this study are listed as follows:

a) The nanoparticle volume fraction of silver (ϕ_2) tends to elevate the velocity and temperature of Ag/KO as well as Ag-$MnZnFe_2O_4$/KO, which are mono and hybrid cases of nanofluids, respectively.
b) The fluid motion and temperature are reduced due to the suction phenomenon. On the other hand, the surface drag got increased with suction for both cases of nanofluids.
c) The heat-transfer rate is an increasing function of Prandtl number, whereas the temperature is decelerated with the effect of Prandtl number.
d) The concentration profile seems to be falling down with an increase in the chemical reaction parameter.
e) The porosity of the medium resists the flow in either case of nanofluids, for example, the pure or hybrid case.

Data availability statement

The raw data supporting the conclusions of this article will be made available by the authors, without undue reservation.

Author contributions

All authors listed have made a substantial, direct, and intellectual contribution to the work and approved it for publication.

Funding

The authors are grateful to the Deanship of Scientific Research, Islamic University of Madinah, Ministry of Education, KSA, for supporting this research work through a research project grant under Research Group Program/1/804.

Conflict of interest

The authors declare that the research was conducted in the absence of any commercial or financial relationships that could be construed as a potential conflict of interest.

Publisher's note

All claims expressed in this article are solely those of the authors and do not necessarily represent those of their affiliated organizations or those of the publisher, the editors, and the reviewers. Any product that may be evaluated in this article or claim that may be made by its manufacturer is not guaranteed or endorsed by the publisher.

References

Abdal, S., Habib, U., Siddique, I., Akgül, A., and Ali, B. (2021). Attribution of multi-slips and bioconvection for micropolar nanofluids transpiration through porous medium over an extending sheet with PST and PHF conditions. *Int. J. Appl. Comput. Math.* 7 (6), 235. doi:10.1007/s40819-021-01137-9

Adnan, Ashraf, W., Khan, I., and Andualem, M. (2022a). Thermal transport investigation and shear drag at solid-liquid interface of modified permeable radiative-SRID subject to Darcy-Forchheimer fluid flow composed by γ-nanomaterial. *Sci. Rep.* 12, 3564. doi:10.1038/s41598-022-07045-2

Adnan, Ashraf, W., Khan, I., Shemseldin, M. A., and Mousa, A. A. A. (2022c). Numerical energy storage efficiency of MWCNTs-Propylene Glycol by inducing thermal radiations and combined convection effects in the constitutive model. *Front. Chem.* 10, 879276. doi:10.3389/fchem.2022.879276

Adnan, Ashraf, W., Khan, U., Al-Johani, A. S., Ahmed, N., Mohyud-Din, S. T., et al. (2022b). Impact of freezing temperature (Tfr) of Al2O3 and molecular diameter (H2O)d on thermal enhancement in magnetized and radiative nanofluid with mixed convection. *Sci. Rep.* 12, 703. doi:10.1038/s41598-021-04587-9

Adnan, Khan, U., Ahmed, N., Mohyud-Din, S. T., Alharbi, S. O., and Khan, I. (2022d). Thermal improvement in magnetized nanofluid for multiple shapes nanoparticles over radiative rotating disk. *Alexandria Eng. J.* 61 (3), 2318–2329. doi:10.1016/j.aej.2021.07.021

Adnan, Khan, U., Ahmed, N., Mohyud-Din, S. T., Alsulami, M. D., and Khan, I. (2022e). A novel analysis of heat transfer in the nanofluid composed by nanodimaond and silver nanomaterials: Numerical investigation. *Sci. Rep.* 12, 1284. doi:10.1038/s41598-021-04658-x

Adnan, Murtaza, R., Hussain, I., Rehman, Z., Khan, I., and Andualem, M. (2022f). Thermal enhancement in Falkner-Skan flow of the nanofluid by considering molecular diameter and freezing temperature. *Sci. Rep.* 12, 9415. doi:10.1038/s41598-022-13423-7

Ahmad, S., Akhter, S., and Shahid, M. I. (2022). Novel thermal aspects of hybrid nanofluid flow comprising of Manganese zinc ferrite $MnZnFe_2O_4$, Nickel zinc ferrite $NiZnFe_2O_4$ and motile microorganisms. *Ain Shams Eng. J.* 13 (5), 101668. doi:10.1016/j.asej.2021.101668

Ahmad, S., Ali, K., Ahmad, S., and Cai, J. (2021). Numerical study of lorentz force interaction with micro structure in channel flow. *Energies* 14 (14), 4286. doi:10.3390/en14144286

Ahmad, S., Ali, K., and Ashraf, M. (2021). MHD flow of Cu-Al2O3/water hybrid nanofluid through a porous media. *J. Por. Media* 24 (7), 61–73. doi:10.1615/JPorMedia.2021036704

Ahmad, S., Ali, K., Faridi, A. A., and Ashraf, M. (2021). Novel thermal aspects of hybrid nanoparticles Cu-TiO2 in the flow of Ethylene Glycol. *Int. Commun. Heat. Mass Transf.* 129, 105708. doi:10.1016/j.icheatmasstransfer.2021.105708

Ahmad, S., Ali, K., Nisar, K. S., Faridi, A. A., Khan, N., Jamshed, W., et al. (2021). Features of Cu and TiO2 in the flow of engine oil subject to thermal jump conditions. *Sci. Rep.* 11, 19592. doi:10.1038/s41598-021-99045-x

Ahmad, S., Ali, K., Rizwan, M., and Ashraf, M. (2021). Heat and mass transfer attributes of copper-aluminum oxide hybrid nanoparticles flow through a porous medium. *Case Stud. Therm. Eng.* 25, 100932. doi:10.1016/j.csite.2021.100932

Ahmad, S., Ashraf, M., and Ali, K. (2021). Simulation of thermal radiation in a micropolar fluid flow through a porous medium between channel walls. *J. Therm. Anal. Calorim.* 144 (3), 941–953. doi:10.1007/s10973-020-09542-w

Ahmad, S., Younis, J., Ali, K., Rizwan, M., Ashraf, M., and Abd El Salam, M. A. (2022). Impact of swimming gyrotactic microorganisms and viscous dissipation on nanoparticles flow through a permeable medium: A numerical assessment. *J. Nanomater.* 2022, 1–11. doi:10.1155/2022/4888128

Ahmed, N., Abbasi, A., Khan, U., and Mohyud-Din, S. T. (2018). Thermal radiation effects on flow of Jeffery fluid in converging and diverging stretchable channels. *Neural Comput. Applic.* 30, 2371–2379. doi:10.1007/s00521-016-2831-5

Ahmed, N., Adnan, Khan, U., Mohyud-Din, S. T., and Manzoor, R. (2017). Influence of viscous dissipation on a copper oxide nanofluid in an oblique channel: Implementation of the KKL model. *Eur. Phys. J. Plus* 132, 237. doi:10.1140/epjp/i2017-11504-y

Ahmed, N., Adnan, Khan, U., and Mohyud-Din, S. T. (2020). Modified heat transfer flow model for SWCNTs-H2O and MWCNTs-H2O over a curved stretchable semi infinite region with thermal jump and velocity slip: A numerical simulation. *Phys. A Stat. Mech. its Appl.* 545, 123431. doi:10.1016/j.physa.2019.123431

Ahmed, N., Adnan, Khan, U., Mohyud-Din, S. T., and Suat Erturk, V. S. (2017). Influence of thermal and concentration gradients on unsteady flow over a stretchable surface. *Results Phys.* 7, 3153–3162. doi:10.1016/j.rinp.2017.08.034

Akhter, S., Ahmad, S., and Ashraf, M. (2022). Cumulative impact of viscous dissipation and heat generation on MHD Darcy-Forchheimer flow between two stretchable disks: Quasi linearization technique. *J. Sci. Arts* 22 (1), 219–232. doi:10.46939/J.Sci.Arts-22.1-c01

Ali, K., Faridi, A. A., Ahmad, S., Jamshed, W., Khan, N., and Alam, M. M. (2022). Quasi-linearization analysis for heat and mass transfer of magnetically driven 3rd-grade (Cu-TiO2/engine oil) nanofluid via a convectively heated surface. *Int. Commun. Heat Mass Transf.* 135, 106060. doi:10.1016/j.icheatmasstransfer.2022.106060

Ayub, R., Ahmad, S., Ahmad, S., Akhtar, Y., Alam, M. M., and Mahmoud, O. (2022). Numerical assessment of dipole interaction with the single-phase nanofluid flow in an enclosure: A pseudo-transient approach. *Materials* 15, 2761. doi:10.3390/ma15082761

Das, S., Tarafdar, B., Jana, R. N., and Makinde, O. D. (2019). Magnetic ferro-nanofluid flow in a rotating channel containing darcian porous medium considering induced magnetic field and Hall currents. *Spec. Top. Rev. Porous Media* 10 (4), 357–383. doi:10.1615/SpecialTopicsRevPorousMedia.2019028377

Dastvareh, B., and Azaiez, J. (2017). Instabilities of nanofluid flow displacements in porous media. *Phys. Fluids* 29, 044101. doi:10.1063/1.4978890

Dawar, A., Islam, S., and Shah, Z. (2022). A comparative analysis of the performance of magnetised copper-copper oxide/water and copper-copper oxide/kerosene oil hybrid nanofluids flowing through an extending surface with velocity slips and thermal convective conditions. *Int. J. Ambient Energy*, 1–19. doi:10.1080/01430750.2022.2063387

Elbashbeshy, E. M. A., and Asker, H. G. (2022). Fluid flow over a vertical stretching surface within a porous medium filled by a nanofluid containing gyrotactic microorganisms. *Eur. Phys. J. Plus* 137, 541. doi:10.1140/epjp/s13360-022-02682-y

Ezhil, K., Thavada, S. K., and Ramakrishna, S. B. (2021). MHD slip flow and heat transfer of Cu-Fe3O4/Ethylene glycol-based hybrid nanofluid over a stretching surface. *Biointerface Res. Appl. Chem.* 11 (4), 11956–11968. doi:10.33263/BRIAC114.1195611968

Jamshed., W., Baleanu, D., Nasir, N. A. A. M., Shahzad, F., Nisar, K. S., Shoaib, M., et al. (2021). The improved thermal efficiency of Prandtl-eyring hybrid nanofluid via classical keller box technique. *Sci. Rep.* 11, 23535. doi:10.1038/s41598-021-02756-4

Kareem, R. S., and Abdulhadi, A. M. (2020). Effect of MHD and porous media on nanofluid flow with heat transfer: Numerical treatment. *J. Adv. Res. Fluid Mech. Therm. Sci.* 63 (2), 317–328.

Khan, W. A., and Pop, I. (2010). Boundary-layer flow of a nanofluid past a stretching sheet. *Int. J. Heat Mass Transf.* 53, 2477–2483. doi:10.1016/j.ijheatmasstransfer.2010.01.032

Mishra, S. R., and Mathur, P. (2020). Williamson nanofluid flow through porous medium in the presence of melting heat transfer boundary condition: Semi-analytical approach. *Mmms* 17 (1), 19–33. doi:10.1108/MMMS-12-2019-0225

Nisar, K. S., Faridi, A. A., Ahmad, S., Khan, N., Ali, K., Jamshed, W., et al. (2022). Cumulative impact of micropolar fluid and porosity on mhd channel flow: A numerical study. *Coatings* 12, 93. doi:10.3390/coatings12010093

Safdar, R., Jawad, M., Hussain, S., Imran, M., Akgül, A., and Jamshed, W. (2022). Thermal radiative mixed convection flow of MHD Maxwell nanofluid: Implementation of buongiorno's model. *Chin. J. Phys.* 77, 1465–1478. doi:10.1016/j.cjph.2021.11.022

Unyong, B., Vadivel, R., Govindaraju, M., Anbuvithya, R., and Gunasekaran, N. (2022). Entropy analysis for ethylene glycol hybrid nanofluid flow with elastic deformation, radiation, non-uniform heat generation/absorption, and inclined Lorentz force effects. *Case Stud. Therm. Eng.* 30, 101639. doi:10.1016/j.csite.2021.101639

Upreti, H., Pandey, A. K., and Kumar, M. (2021). Assessment of entropy generation and heat transfer in three-dimensional hybrid nanofluids flow due to convective surface and base fluids. *J. Porous Media* 24 (3), 35–50. doi:10.1615/JPorMedia.2021036038

Yahya, A. U., Siddique, I., Jarad, F., Salamat, N., Abdal, S., Hamed, Y. S., et al. (2022). On the enhancement of thermal transport of Kerosene oil mixed TiO2 and SiO2 across Riga wedge. *Case Stud. Therm. Eng.* 34, 102025. doi:10.1016/j.csite.2022.102025

Zahid, M., Asjad, M. I., Hussain, S., and Akgül, A. (2021). Nonlinear magnetohydrodynamic flow of nanofluids across a porous matrix over an extending sheet with mass transpiration and bioconvection. *Heat. Transf.* 50 (8), 7588–7603. doi:10.1002/htj.22244

Zainal, N. A., Nazar, R., Naganthran, K., and Pop, I. (2022). Slip effects on unsteady mixed convection of hybrid nanofluid flow near the stagnation point. *Appl. Math. Mech.-Engl. Ed.* 43, 547–556. doi:10.1007/s10483-022-2823-6

Nomenclature

ρ_{hnf} Density of the hybrid nanofluid
v Component of velocity along the y-axis
σ_{hnf} Electrical conductivity of the hybrid nanofluid
k^* Darcy permeability
v_0 Suction velocity (where $v_0 > 0$)
$C_{p_{hnf}}$ Specific heat of the hybrid nanofluid
u Component of velocity along the x-axis
K_r Rate constant of chemical reaction
k_{hnf} Thermal conductivity of the hybrid nanofluid
c Stretching/shrinking constant
v_{hnf} Kinematic viscosity of the hybrid nanofluid
T Temperature of the fluid
μ_{hnf} Hybrid nanofluid viscosity
T_∞ Temperature far away from the sheet
C Concentration of the fluid
T_w Fixed temperature at the surface
D_B Diffusion coefficient
C_∞ Concentration far away from the sheet